Supplemental Material

SM $e^-\gamma \to e^-\gamma$ in the forward limit: We perform an explicit calculation of the amplitude $\mathcal{M}(e^-\gamma \to e^-\gamma)$ in SM in the forward limit with massless electrons. Our calculation follow closely Sec 5.5 of Ref. [1]. The general amplitude is given by

$$i\mathcal{M} = -ie^2\epsilon^*_\mu(k')\epsilon_\nu(k)\bar{u}(p')\left[\frac{\gamma^\mu(\not{p}+\not{k})\gamma^\nu}{(p+k)^2} + \frac{\gamma^\nu(\not{p}-\not{k}')\gamma^\mu}{(p-k')^2}\right]u(p)\,, \tag{1}$$

where p, k, p' and k' are the momenta of the ingoing e^-, γ and the outgoing e^-, γ, respectively, as shown in Figure 1. We assume that both e^- and γ have + helicity (right-handed). It can be shown that the results are the same for the other helicity configurations. To calculate the amplitude in the forward limit, it is most convenient to choose a particular reference frame and a basis for the spinors. We choose the initial (and final) momenta to be along the z-axis, as shown in Figure 2. The Dirac matrices are given by

$$\gamma^\mu = \begin{pmatrix} 0 & \sigma^\mu \\ \bar{\sigma}^\mu & 0 \end{pmatrix}\,, \quad \text{where} \quad \sigma^\mu = (1,\vec{\sigma})\,, \quad \bar{\sigma}^\mu = (1,-\vec{\sigma})\,. \tag{2}$$

Since we have chosen e^- and γ to be right-handed, we have for the Dirac spinor

$$u(p) = \begin{pmatrix} 0 \\ u_R(p) \end{pmatrix} \quad \text{where} \quad u_R(p) = u_R(p') = \sqrt{2E}\begin{pmatrix} 0 \\ 1 \end{pmatrix}\,, \tag{3}$$

following the spinor choice in Ref. [1]. This also gives

$$\bar{u}(p')\gamma^\mu = u^\dagger(p')\gamma^0\gamma^\mu = \begin{pmatrix} 0 & u^\dagger_R(p)\sigma^\mu \end{pmatrix}\,. \tag{4}$$

The polarization vector are given by

$$\epsilon^\mu = \frac{1}{\sqrt{2}}(0,\ 1,\ i,\ 0)^\mu\,, \quad \epsilon^{*\mu} = \frac{1}{\sqrt{2}}(0,\ 1,\ -i,\ 0)^\mu\,, \tag{5}$$

which gives

$$\sigma^\mu\epsilon_\mu = \begin{pmatrix} 0 & -\sqrt{2} \\ 0 & 0 \end{pmatrix}\,, \quad \sigma^\mu\epsilon^*_\mu = \begin{pmatrix} 0 & 0 \\ -\sqrt{2} & 0 \end{pmatrix}\,. \tag{6}$$

Plugging everything into Equation 1, we have

$$\begin{aligned}\mathcal{M} &= -e^2\epsilon^*_\mu\epsilon_\nu u^\dagger_R\left[\frac{\sigma^\mu\bar{\sigma}\cdot(p+k)\sigma^\nu}{s} + \frac{\sigma^\nu\bar{\sigma}\cdot(p-k')\sigma^\mu}{u}\right]u_R \\ &= -e^2\epsilon^*_\mu\epsilon_\nu 2E\begin{pmatrix} 0 & 1 \end{pmatrix}\left[\begin{pmatrix} 0 & 0 \\ -\sqrt{2} & 0 \end{pmatrix}\frac{2E}{4E^2}\begin{pmatrix} 0 & -\sqrt{2} \\ 0 & 0 \end{pmatrix} + 0\right]\begin{pmatrix} 0 \\ 1 \end{pmatrix} \\ &= -2e^2\,.\end{aligned} \tag{7}$$

Operators: Eq. 8 shows the five dimension-8 operators mentioned in the main text, as defined in Ref. [2]. The lepton flavor indices are omitted as they are not relevant for our study. The Lagrangian is written in the form $\mathcal{L}_{\text{dim-8}} = \sum_i \frac{c_i}{\Lambda^4}Q_i$.

$$\begin{aligned} Q_{l^2B^2D} &= i(\bar{l}\gamma^\mu \overleftrightarrow{D}^\nu l)B_{\mu\rho}B_\nu{}^\rho\,, \\ Q^{(2)}_{l^2WBD} &= i(\bar{l}\gamma^\mu\tau^I \overleftrightarrow{D}^\nu l)(B_{\mu\rho}W^{I\rho}_\nu + B_{\nu\rho}W^{I\rho}_\mu)\,, \\ Q^{(1)}_{l^2W^2D} &= i(\bar{l}\gamma^\mu \overleftrightarrow{D}^\nu l)W^I_{\mu\rho}W^{I\rho}_\nu\,, \\ Q_{e^2B^2D} &= i(\bar{e}\gamma^\mu \overleftrightarrow{D}^\nu e)B_{\mu\rho}B_\nu{}^\rho\,, \\ Q_{e^2W^2D} &= i(\bar{e}\gamma^\mu \overleftrightarrow{D}^\nu e)W^I_{\mu\rho}W^{I\rho}_\nu\,. \end{aligned} \tag{8}$$

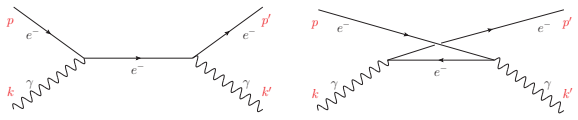

FIG. 1: Feynman diagrams for $e^-\gamma \to e^-\gamma$ in the SM.

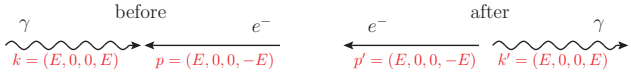

FIG. 2: Momenta of the forward scattering process before and after the collision.

Differential cross section: Figure 3 shows the differential cross section $d\sigma/d|\cos\theta|$ for the SM and the d8 contribution for $\sqrt{s} = 240\,\text{GeV}$, unpolarized beams. The SM contribution dominates in the forward region due to the t/u-channel electron exchange.

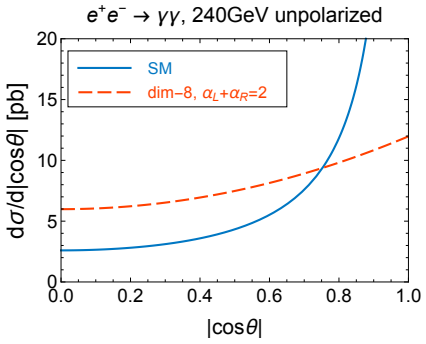

FIG. 3: The differential cross section $d\sigma/d|\cos\theta|$ for the SM and the d8 contribution (as in Eq. (4) in the main text) for $\sqrt{s} = 240\,\text{GeV}$, unpolarized beams. For the d8 contribution, an arbitrary benchmark of $a_L + a_R = 2$ is chosen.

Run scenarios: Table I is a summary of the run scenarios of future lepton colliders considered in our analysis, with the corresponding integrated luminosity. For ILC and CLIC, the numbers in the brackets are the values of beam polarizations $P(e^-, e^+)$. For simplicity, we assume the Z-pole or WW-threshold runs are at one single energy. Numbers are taken from Refs. [3, 4]. Further details can be found in Refs. [5–10].

$\int \mathcal{L}dt$ [ab^{-1}]				
unpolarized	91 GeV	161 GeV	240 GeV	365 GeV
CEPC	8	2.6	5.6	
FCC-ee	150	10	5	1.5
ILC	250 GeV	350 GeV	500 GeV	
$(-0.8, +0.3)$	0.9	0.135	1.6	
$(+0.8, -0.3)$	0.9	0.045	1.6	
$(\pm 0.8, \pm 0.3)$	0.1	0.01	0.4	
CLIC	380 GeV	1.5 TeV	3 TeV	
$(-0.8, 0)$	0.5	2	4	
$(+0.8, 0)$	0.5	0.5	1	
muon collider	10 TeV	30 TeV		
unpolarized	10	90		

TABLE I: A summary of the run scenarios of future lepton colliders considered in our analysis with the corresponding integrated luminosity.

Measurement uncertainties: We have only considered statistical uncertainties in our analysis. Here we provide further verifications of this assumption. Figure 4 shows the total cross sections of diphoton process and the main background from Bhabha scattering ($e^+e^- \to e^+e^-$), the latter contributes to the diphoton channel if both final state particles mistagged as a photon. Even with a conservative 1% mistag rate for both electrons and positrons, this background is more than two orders of magnitude smaller than the signal. This is consistent with the LEP analysis in *e.g.* Ref. [11], which stated that the contamination from the major background, Bhabha events, was estimated to be less than 0.5% after selection cuts. Another potential source of background is the double-hard-FSR: $e^+e^- \to e^+e^-\gamma\gamma$, where the two photons take most of the energy of the scattered electrons. Applying $m_{\gamma\gamma} \geq 0.9s$ on the invariant mass of the two photons with other reasonable cuts, we estimate the cross section of this process to be $6 \sim 7$ orders of magnitude lower than the signal process. The statistical uncertainties of the total diphoton cross section measurements are provided for each collider scenario in Table II as references.

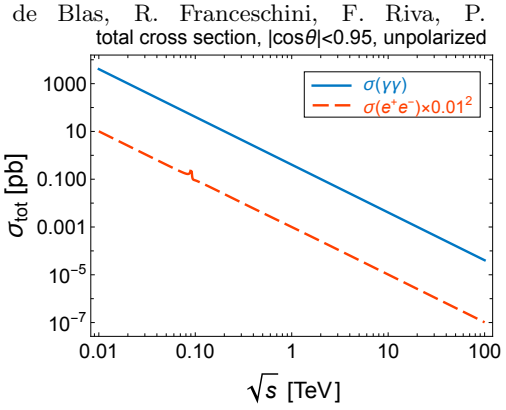

FIG. 4: The total cross sections of $e^+e^- \to \gamma\gamma$ and the main background from $e^+e^- \to e^+e^-$ with both final state particles mistagged as a photon. A cut on the production polar angle $|\cos\theta| < 0.95$ is applied. A conservative 1% mistag rate is assumed for both electrons and positrons.

$\Delta\sigma_{\rm tot}/\sigma_{\rm tot}$, $e^+e^- \to \gamma\gamma$				
unpolarized	91 GeV	161 GeV	240 GeV	365 GeV
CEPC	5.1×10^{-5}	1.6×10^{-4}	1.6×10^{-4}	
FCC-ee	1.2×10^{-5}	8.0×10^{-5}	1.7×10^{-4}	4.7×10^{-4}
ILC	250 GeV	350 GeV	500 GeV	
	2.5×10^{-4}	1.1×10^{-3}	3.7×10^{-4}	
CLIC	380 GeV	1.5 TeV	3 TeV	
	6.0×10^{-4}	1.5×10^{-3}	2.1×10^{-3}	
muon collider	10 TeV	30 TeV		
	5.0×10^{-3}	5.0×10^{-3}		

TABLE II: The projected (relative) statistical uncertainties of the total cross section measurement of $e^+e^- \to \gamma\gamma$ with the run scenarios in Table I. A cut on the production polar angle $|\cos\theta| < 0.95$ is applied.

[1] M. E. Peskin and D. V. Schroeder, *An Introduction to quantum field theory* (Addison-Wesley, Reading, USA, 1995), ISBN 978-0-201-50397-5.
[2] C. W. Murphy, JHEP **10**, 174 (2020), 2005.00059.
[3] J. De Blas, G. Durieux, C. Grojean, J. Gu, and A. Paul, JHEP **12**, 117 (2019), 1907.04311.
[4] T. Han, D. Liu, I. Low, and X. Wang (2020), 2008.12204.
[5] M. Dong et al. (CEPC Study Group) (2018), 1811.10545.
[6] A. Abada et al. (FCC), Eur. Phys. J. C **79**, 474 (2019).
[7] A. Abada et al. (FCC), Eur. Phys. J. ST **228**, 261 (2019).
[8] P. Bambade et al. (2019), 1903.01629.
[9] J. de Blas, R. Franceschini, F. Riva, P. Roloff, U. Schnoor, M. Spannowsky, J. Wells, A. Wulzer, J. Zupan, et al., **3/2018** (2018), 1812.02093.
[10] J. P. Delahaye, M. Diemoz, K. Long, B. Mansoulié, N. Pastrone, L. Rivkin, D. Schulte, A. Skrinsky, and A. Wulzer (2019), 1901.06150.
[11] M. Acciarri et al. (L3), Phys. Lett. B **353**, 136 (1995).